Growing Correlation Length on Cooling Below the Onset of Caging in a Simulated Glass-Forming Liquid

N. Lačević[1,2,3], F.W. Starr[2], T.B. Schrøder[2,4], V.N. Novikov[2,*] and S.C. Glotzer[1,2]
[1] *Departments of Chemical Engineering and Materials Science and Engineering, University of Michigan, Ann Arbor, MI 48109, USA*
[2] *Center for Theoretical and Computational Materials Science and Polymers Division, National Institute of Standards and Technology, Gaithersburg, MD 20899, USA*
[3] *Department of Physics and Astronomy, Johns Hopkins University Baltimore, MD 21210, USA and*
[4] *IMFUFA, Roskilde University, DK-4000, Denmark*
(Dated: June 18, 2002)

We present a calculation of a fourth-order, time-dependent density correlation function that measures higher-order spatiotemporall correlations of the density of a liquid. From molecular dynamics simulations of a glass-forming Lennard-Jones liquid, we find that the characteristic length scale of this function has a maximum as a function of time which increases steadily beyond the characteristic length of the static pair correlation function $g(r)$ in the temperature range approaching the mode coupling temperature from above.

PACS numbers: PACS numbers: 64.70.pf, 61.20.lc

Relaxation in liquids near their glass transition involves the correlated motion of groups of neighboring particles [1, 2, 3]. This correlated motion results in spatially heterogeneous dynamics, which becomes increasingly heterogeneous as the liquid is cooled. Much remains to be understood regarding the nature of this heterogeneity, and how to best measure and quantify it. The traditional two-point, time-dependent, van Hove density correlation function $G(r,t)$, provides information about the transient "caging" of particles on cooling [4], but does not provide local information about correlated motion and dynamical heterogeneity. In particular, the static correlation length associated with two-point density fluctuations remains relatively constant upon cooling [5, 6]. Instead, other correlation functions, which involve, e.g., spatial correlations of the displacements of particles in the liquid, and other measures of correlated motion, have been used to demonstrate the heterogeneous nature of the liquid dynamics in molecular dynamics (MD) simulations [7, 8]. These "measures" are readily accessible in colloidal suspensions, where microscopy provides detailed information on particle trajectories similar to the information obtained from MD simulations. Indeed, such experiments have confirmed simulation predictions of increasingly heterogeneous dynamics near the glass transition [9].

In this paper, we evaluate a fourth-order, time-dependent density correlation function $g_4(r,t)$ that is more sensitive to spatially heterogeneous dynamics than $G(r,t)$. This four-point function was first investigated in supercooled liquids by Dasgupta et al. [10], but they did not detect a growing correlation length in their simulations. Recently, it was shown [11, 12] that it is possible to define a generalized, time-dependent susceptibility $\chi_4(t)$ which (i) is proportional to the volume integral of $g_4(r,t)$ in the same way that the isothermal compressibility is related to the volume integral of the static pair correlation function [13], (ii) is non-zero in the caging regime, and (iii) increases with decreasing T. While this indirectly suggests the presence of a growing correlation length, neither $g_4(r,t)$ nor its range $\xi_4(t)$ was calculated in those works. Here we calculate $g_4(r,t)$ in a simulation of 8000 Lennard-Jones (LJ) particles, and show that $\xi_4(t)$ grows slowly but steadily beyond the correlation length ξ of the static pair correlation function $g(r)$ as temperature T is decreased from the onset of caging towards the mode coupling temperature $T_{\rm MCT}$ [4].

We first briefly review the general theoretical framework, some of which was previously discussed in Refs. [11, 12, 14], and extend it to obtain a form for $g_4(r,t)$ suitable for calculation in our simulations. Consider a liquid of N particles occupying a volume V, with density $\rho(\mathbf{r},t) = \sum_{i=1}^{N} \delta(\mathbf{r} - \mathbf{r}_i(t))$. Extending an idea originally proposed for spin glasses [15], one may construct a time-dependent 'order parameter' that compares the liquid configuration at two different times [11, 12, 14]:

$$Q(t) = \int d\mathbf{r}_1 d\mathbf{r}_2 \rho(\mathbf{r}_1,0)\rho(\mathbf{r}_2,t) w(|\mathbf{r}_1 - \mathbf{r}_2|) = \sum_{i=1}^{N}\sum_{j=1}^{N} w(|\mathbf{r}_i(0) - \mathbf{r}_j(t)|). \quad (1)$$

* Permanent address: Institute of Automation and Electrometry, Russian Academy of Science, Novosibirsk, 630090, Russia

Here, $\mathbf{r}_i$ in the second equality refers to the position of particle i, and $w(|\mathbf{r}_i - \mathbf{r}_j|)$ is an "overlap" function which is unity for $|\mathbf{r}_i - \mathbf{r}_j| \leq a$ and zero otherwise, where the parameter a is associated with the typical vibrational amplitude of the particles[11, 12]. For the present work, we take $a = 0.3$ particle diameters as in Refs. [11, 12], since this value maximizes the effect studied here [16]. As defined, $Q(t)$ is the number of "overlapping" particles when configurations of the system at $t = 0$ and at a later time t are compared; that is, $Q(t)$ counts the number of particles that either remain within a distance a of their original position, or are replaced (within a distance a) by another particle in an interval t.

The fluctuations in $Q(t)$ are described by a generalized susceptibility

$$\chi_4(t) = \frac{\beta V}{N^2}\Big(\langle Q^2(t)\rangle - \langle Q(t)\rangle^2\Big), \tag{2}$$

where $\beta = 1/k_B T$, k_B is Boltzmann's constant, and $\langle \cdots \rangle$ indicates an ensemble average as in Ref. [12]. Note that at very early times, when $Q(t) = N$ because no particle has yet moved beyond a distance a, $\chi_4(t)$ is identical to the isothermal compressibility κ_T [17]. Substituting Eq. (1) into Eq. (2), we obtain

$$\chi_4(t) = \frac{\beta V}{N^2} \int d\mathbf{r}_1 d\mathbf{r}_2 d\mathbf{r}_3 d\mathbf{r}_4 \, G_4(\mathbf{r}_1, \mathbf{r}_2, \mathbf{r}_3, \mathbf{r}_4, t), \tag{3}$$

where

$$\begin{aligned} G_4(\mathbf{r}_1, \mathbf{r}_2, \mathbf{r}_3, \mathbf{r}_4, t) &= \langle \rho(\mathbf{r}_1, 0)\rho(\mathbf{r}_2, t) w(|\mathbf{r}_1 - \mathbf{r}_2|)\rho(\mathbf{r}_3, 0)\rho(\mathbf{r}_4, t) w(|\mathbf{r}_3 - \mathbf{r}_4|)\rangle \\ &- \langle \rho(\mathbf{r}_1, 0)\rho(\mathbf{r}_2, t) w(|\mathbf{r}_1 - \mathbf{r}_2|)\rangle \langle \rho(\mathbf{r}_3, 0)\rho(\mathbf{r}_4, t) w(|\mathbf{r}_3 - \mathbf{r}_4|)\rangle. \end{aligned} \tag{4}$$

As written, G_4 is a function of four spatial and two temporal coordinates, constrained in a particular way by the overlap functions. To investigate the behavior of G_4, we consider a function $g_4(r, t)$ such that $\chi_4(t) = \beta \int d\mathbf{r} \; g_4(r, t)$. We integrate first over $\mathbf{r}_2$ and $\mathbf{r}_4$ in Eq. (3), define $\mathbf{r} \equiv \mathbf{r}_3 - \mathbf{r}_1$, and then integrate over $\mathbf{r}_3$ to obtain

$$g_4(r, t) = \Big\langle \frac{1}{N\rho} \sum_{ijkl} \delta(\mathbf{r} - \mathbf{r}_k(0) + \mathbf{r}_i(0)) w(|\mathbf{r}_i(0) - \mathbf{r}_j(t)|) w(|\mathbf{r}_k(0) - \mathbf{r}_l(t)|) \Big\rangle - \Big\langle \frac{Q(t)}{N} \Big\rangle^2 \tag{5}$$

We investigate the behavior of $g_4(r, t)$, which is the angular averaged function of a single variable $\mathbf{r}$. With the above choice of integration variables, $g_4(r, t)$ describes spatial correlations between overlapping particles at the initial time (using information at time t to label the overlapping particles). The first term in $g_4(r, t)$ is a pair correlation function restricted to the subset of overlapping particles, $g_4^{\rm ol}(r, t)$. The second term represents the "bulk" probability of any two particles overlapping. We can rewrite $g_4(r, t)$ as

$$\begin{aligned} g_4(r, t) &= g_4^{\rm ol}(r, t) - \Big\langle \frac{Q(t)}{N} \Big\rangle^2 = \Big\langle \frac{Q(t)}{N} \Big\rangle^2 \Big[\frac{g_4^{\rm ol}(r, t)}{\langle \frac{Q(t)}{N} \rangle^2} - 1 \Big] \\ &\equiv \Big\langle \frac{Q(t)}{N} \Big\rangle^2 g_4^*(r, t). \end{aligned} \tag{6}$$

Since $\langle \frac{Q(t)}{N} \rangle$ is a function of time, information about spatial correlations is contained in $g_4^*(r, t)$, which we investigate in the rest of the paper. In comparing $g_4(r, t)$ with other correlation functions used to study glass-forming liquids, we note that neutron scattering studies, such as those by Colmenero and Richter and coworkers on polymer systems [18], measure at most two-point spatiotemporal density correlation functions. 4-D NMR methods used to probe dynamical heterogeneity measure multiple time correlation functions [19]. In contrast to those, $g_4(r, t)$ contains additional, higher order spatiotemporal information.

To evaluate $g_4^*(r, t)$, we perform MD simulations of a model LJ glass-forming liquid. The system is a three-dimensional (50:50) binary mixture of 8000 particles interacting via LJ interaction parameters [12, 20]. We simulate eight state points in the microcanonical ensemble at fixed density $\rho = 1.29$, in a temperature range $0.59 - 2.0$; we estimate $T_{\rm MCT} = 0.57 \pm 0.02$ and the Vogel-Fulcher temperature $T_0 = 0.48 \pm 0.02$. The error bars are confidence intervals obtained as a result of fitting $\tau_\alpha(T)$ to a power law and exponential form, respectively. The onset of caging and non-exponential relaxation of the intermediate scattering function occur at $T_{\rm cage} \approx 1.0$. Our simulations thus span a range that includes the onset of caging and the initial slowing down of the liquid approaching $T_{\rm MCT}$. The isochore along which the simulations are performed was chosen to reproduce simulations of a smaller system size performed earlier, which showed (i) that this model exhibits spatially heterogeneous dynamics[12], and (ii) that transitions between inherent structures close to $T_{\rm MCT}$ occur through the collective, quasi-one-dimensional motion of strings of

particles [21]. All data evaluated in the present work are in thermodynamic equilibrium above the glass transition temperature.

We plot $g_4^*(r,t)$ for several t at our second coldest temperature $T = 0.60$ in Figs. 1(a) and (b). The positions of the peaks in $g_4^*(r,t)$ are identical to the positions of the peaks in $g(r)$ (not shown). We confirm that $g_4^*(r,t) = g(r) - 1$ in the ballistic and diffusive regime. Note that in the diffusive regime $g_4^{\rm o|}(r,t)$ is the pair correlation function of the random overlaps normalized by $\langle \frac{Q(t)}{N} \rangle^2$ to yield $g(r)$. We plot $\chi_4(t)$ and $\langle \frac{Q(t)}{N} \rangle$ at $T = 0.60$ in Fig. 1(c); as found in Refs. [11, 12], $\chi_4(t)$ has a maximum at an intermediate time t_4^*. Refs. [11, 12] showed that this maximum increases and shifts to longer time as T decreases toward $T_{\rm MCT}$, and we further find that t_4^* is in the α-relaxation regime at each T. $g_4^*(r,t)$ deviates from $g(r)-1$ when $\langle \frac{Q(t)}{N} \rangle$ deviates from unity and $\chi_4(t)$ becomes non-zero[22]. The amplitude and range of $g_4^*(r,t)$ increase with increasing t until a time t_4^*. At t_4^*, $g_4^*(r,t_4^*)$ (indicated by the solid curve in Figs. 1(a,b)) exhibits a long tail which decreases slowly to zero with increasing distance. For t greater than t_4^*, the amplitude and range of $g_4^*(r,t)$ decrease, and $g_4^*(r,t) = g(r) - 1$ when $\chi_4(t)$ decays to zero (not shown). The positions of the peaks in $g_4^*(r,t)$ do not appear to change with decreasing T.

Fig. 2 shows the T dependence of $g_4^*(r,t)$ at the peak characteristic time t_4^* when the correlations at each T are most pronounced, as measured by $\chi_4(t)$. The inset of Fig. 2 shows the "four-point" structure factor $S_4^*(q,t_4^*) = \rho \int d\mathbf{r} g_4^*(r,t_4^*) \sin(qr)/qr$, and static structure factor $S(q) - 1 = \rho \int d\mathbf{r}[g(r) - 1] \sin(qr)/qr$. We find that while $S(q)$ shows no change at small q, $S_4(q,t_4^*)$ develops a peak at small q that grows with decreasing T, indicating a growing range of correlations.

Fig. 3 provides a close-up of the behavior of $g_4^*(r,t_4^*)$ for $1.7 < r < 7$, for several values of T. To extract a value for $\xi_4(t)$, we fit peaks of $g_4^*(r,t)$ in the range shown to the exponential function $y(r) = a * \exp(-{\rm r}/\xi_4({\rm t}))$. We refer to this method as an "envelope fit". The time dependence of $\xi_4(t)$ obtained from this fit is plotted for several state points in Fig. 4. We see that the qualitative behavior of $\xi_4(t)$ is similar to that of $\chi_4(t)$: $\xi_4(t)$ has a maximum in time, and as T decreases, the amplitude and time of this maximum increase.

The length scale $\xi_4(t)$ characterizes the typical distance over which "overlapping" particles are spatially correlated, and includes contributions from the static two-point density correlations. At temperatures above the onset of caging, where the dynamics is everywhere homogeneous, $\xi_4(t_4^*)$ and ξ coincide. Below the onset of caging, $\xi_4(t_4^*)$ begins to grow larger than ξ; over the limited T-range of our simulations, we find that $\xi_4(t)$ increases from 0.8 ± 0.1 particle diameters above $T_{\rm cage}$ to 1.5 ± 0.1 particle diameters within 5% of $T_{\rm MCT}$ (Fig. 4 inset). In contrast, we find that ξ, which is coincident with $\xi_4(t)$ at short times when $\langle \frac{Q(t)}{N} \rangle = 1$, changes less, from 0.8 ± 0.1 to 1.1 ± 0.1 particle diameters. Thus, over the T-range studied, the characteristic distance over which particle motion is most correlated *grows to exceed the static correlation length*. While we cannot reliably predict the behavior of $\xi_4(t_4^*)$ at lower T, we find no tendency for slowing down of its growth, unlike the low-T behavior of ξ which is known to remain finite and small. We do observe a slight depression of $\xi_4(t)$ and $\chi_4(t)$ at our lowest $T = 0.59$ (not shown), but we speculate this may be due to finite size effects, which we will explore in detail in a later publication.

The relatively small but growing correlation length calculated here from the four-point spatiotemporal density correlation function should be contrasted with that characterizing the size of highly mobile regions within the fluid [7]. That length was shown to grow much more rapidly on cooling, approaching the size of the simulation box close to $T_{\rm MCT}$. Interestingly, whereas the correlation length of highly mobile regions was found to be largest on a time scale in the β-relaxation regime, the length calculated in the present paper is largest in the α-regime. We note that $g_4(r,t)$ is dominated by "caged" particles, and thus $\xi_4(t)$ may be related to length scales calculated in Ref. [23]. The relationship of the different length scales characterizing dynamical heterogeneity will be explored in a subsequent publication.

[1] H. Sillescu, J. Non-Cryst. Solids **243**, 81 (1999).
[2] M. D. Ediger, Annu. Rev. Phys. Chem. **51**, 99 (2000).
[3] S. C. Glotzer, J. Non-Cryst. Solids **274**, 342 (2000).
[4] W. Götze, L. Sjögren, Rep. Prog. Phys. **55**, 241 (1992).
[5] M. R. Ernst, et al., Phys. Rev. B **43**, 8070 (1991).
[6] R. L. Leheny, et al, J. Chem Phys. **105**, 7783 (1996); A. van Blaaderen and P. Wiltzius, Science **270**, 1177 (1995).
[7] W. Kob, C. Donati, P.H. Poole, S.J. Plimpton and S.C. Glotzer, Phys. Rev. Lett. **79**, 2827 (1997); C. Donati, S.C. Glotzer, and P.H. Poole, Phys. Rev. Lett. **82**, 6064 (1999); C. Donati, et al., Phys. Rev. E **60**, 3107 (1999); C. Bennemann, C. Donati, J. Baschnagel and S. C. Glotzer, Nature **399**, 246 (1999); Y. Gebremichael, T. B. Schrøder, F. W. Starr and S. C. Glotzer, Phys. Rev. E **64**, 51503 (2001).
[8] See e.g., B. Doliwa and A. Heuer, Phys. Rev. E **61**, 6898 (2000); R. Yamamoto and A. Onuki, Phys. Rev. Lett. **81**, 4915 (1998); Phys. Rev. E **58**, 3515 (1998); T. Muranaka and Y. Hiwatari, Phys. Rev. E **51**, R2735 (1995); M. Hurley and P. Harrowell, Phys. Rev. E **52**, 1694 (1995); J. Qian, R. Hentschke and A. Heuer, J. Chem. Phys. **111**, 10177 (1999); A. I.

Mel'cuk, et al. Phys. Rev. Lett. **75**, 2522 (1995); G. Johnson, et al, Phys. Rev. E **57**, 5707 (1998); N. E. Moe and M. D. Ediger, Polymer **37**, 1787 (1996).

[9] W. K. Kegel and A. van Blaaderen, Science **287**, 290 (2000); E. R. Weeks, et al, Science **287**, 627 (2000); S. C. Glotzer, Phys. World **13**, 22 (2000).

[10] C. Dasgupta, A.V. Indrani, S. Ramaswamy and M.K. Phani, Europhys. Lett. **15**, 307 (1991); *ibid* **15**, 467 (1991).

[11] C. Donati, S. Franz, G. Parisi and S. C. Glotzer, cond-mat/9905433.

[12] S. C. Glotzer, V. N. Novikov and T. B. Schrøder, J. Chem. Phys. **112**, 509 (2000).

[13] J. P. Hansen and I. R. McDonald, Theory of Simple Liquids, Academic Press, 1986.

[14] S. Franz, et al, Philosopical Magazine B, **79**, 1827 (1999); S. Franz and G. Parisi, J. Phys.: Condens. Matter **12**, 6335 (2000).

[15] S. Franz and G. Parisi, Phys. Rew. Lett. **79**, 2486 (1997); G. Parisi, Phys. Rev. Lett. **50**, 1946 (1983); S. F. Edwards and P. W. Anderson, J. Phys. F: Metal Phys. **5**, 965 (1975).

[16] N. Lačević, et al, preprint.

[17] H. E. Stanley, Introduction to Phase Transitions and Critical Phenomena, New York, Oxford University Press, 1971.

[18] J. Colmenero et al., Phys. Rev. Lett. **69**, 478 (1992); A. Arbe et al., Phys. Rev. Lett. **81**, 590 (1998).

[19] U. Tracht, et al., Phys. Rev. Lett. **81**, 2727 (1998); H. W. Spiess, Macromolecular Symposia, **117**, 257 (1997); K. Schmidt-Rohr and H. W. Spiess, Phys. Rev. Lett. **66**, 3020 (1991).

[20] The LJ interaction parameters $\epsilon_{\alpha\beta}$ and $\sigma_{\alpha\beta}$ are given by $\epsilon_{AA} = \epsilon_{AB} = \epsilon_{BB} = 1$, $\sigma_{AA} = 1$, $\sigma_{BB} = 5/6$, $\sigma_{AB} = (\sigma_{AA} + \sigma_{BB})/2$. Lengths are defined in units of σ_{AA}, temperature T in units of ϵ_{AA}/k_B, and time in units of $(m_B\sigma_{AA}^2/48\epsilon_{AA})^{1/2}$.

[21] T. B. Schrøder, et al., J. Chem. Phys. **112**, 9834 (2000).

[22] Strictly speaking, a simulation in the grand canonical ensemble would instead yield a small but non-zero $\chi_4(t)$ value at early times.

[23] R. D. Mountain, Supercooled Liquids ACS Symposium **676**, 122 (1997); R. D. Mountain, J. Chem. Phys. **102**, 5408 (1995); R. Ahluwalia and S. P. Das, Phys. Rev. E **57**, 5771 (1997).

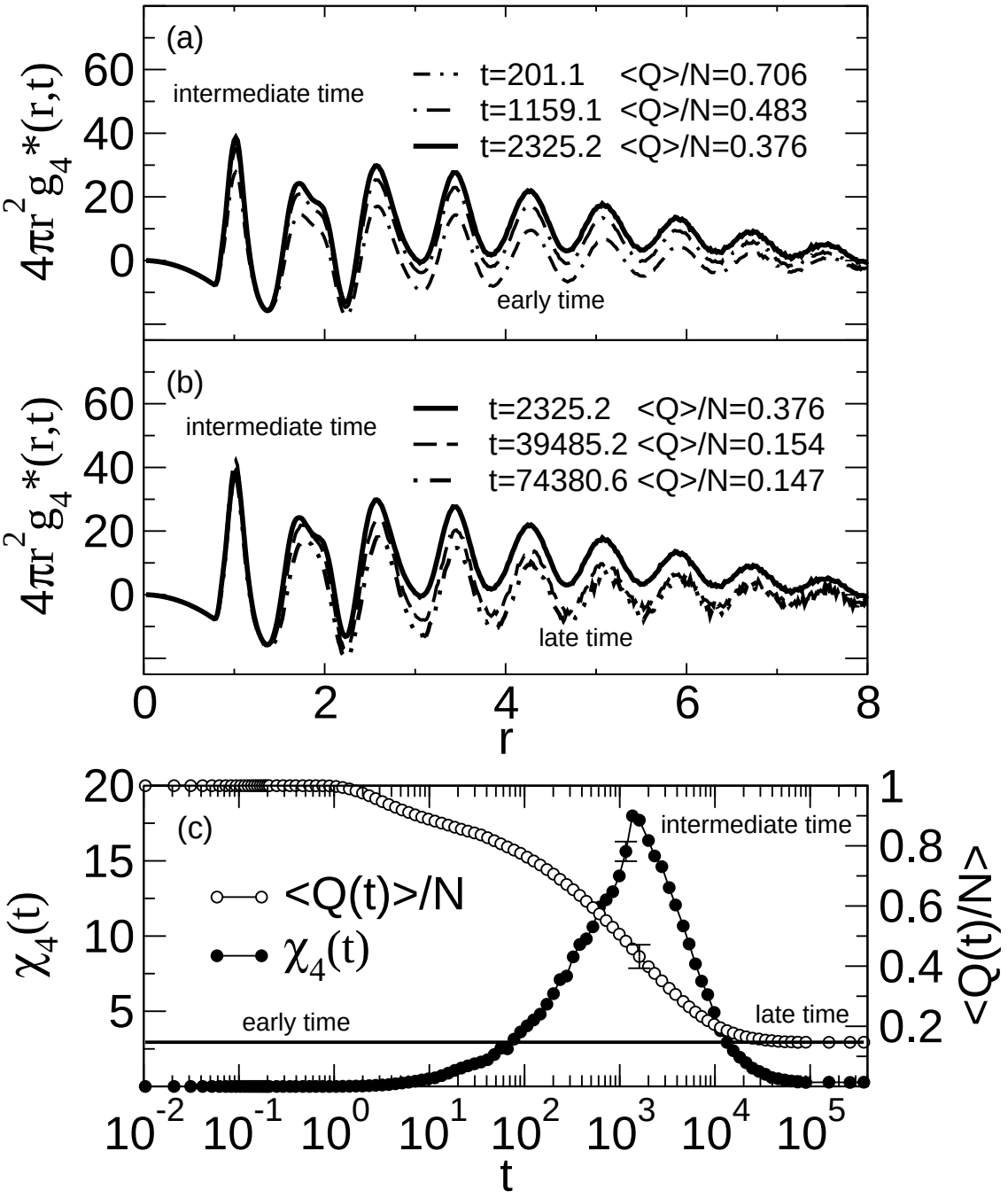

FIG. 1: Time dependence of $g_4^*(r,t)$ at $T = 0.60$, showing (a) the amplitude and range of $g_4^*(r,t)$ growing in time and (b) the amplitude and range of $g_4^*(r,t)$ decaying in time. The fraction $\langle \frac{Q(t)}{N} \rangle$ indicates the average fraction of overlapping particles present at time t. (c) Time dependence of $\chi_4(t)$ and $\langle \frac{Q(t)}{N} \rangle$ at $T = 0.60$. The long time value of $\langle \frac{Q(t)}{N} \rangle = \rho V_a$ (solid line), where $V_a = \frac{4\pi a^3}{3}$ corresponds to the probability of finding a random overlapping particle. The error bars in $Q(t)$ and $\chi_4(t)$ are calculated by averaging over 100 successive independent blocks, and are representative of the error in all points.

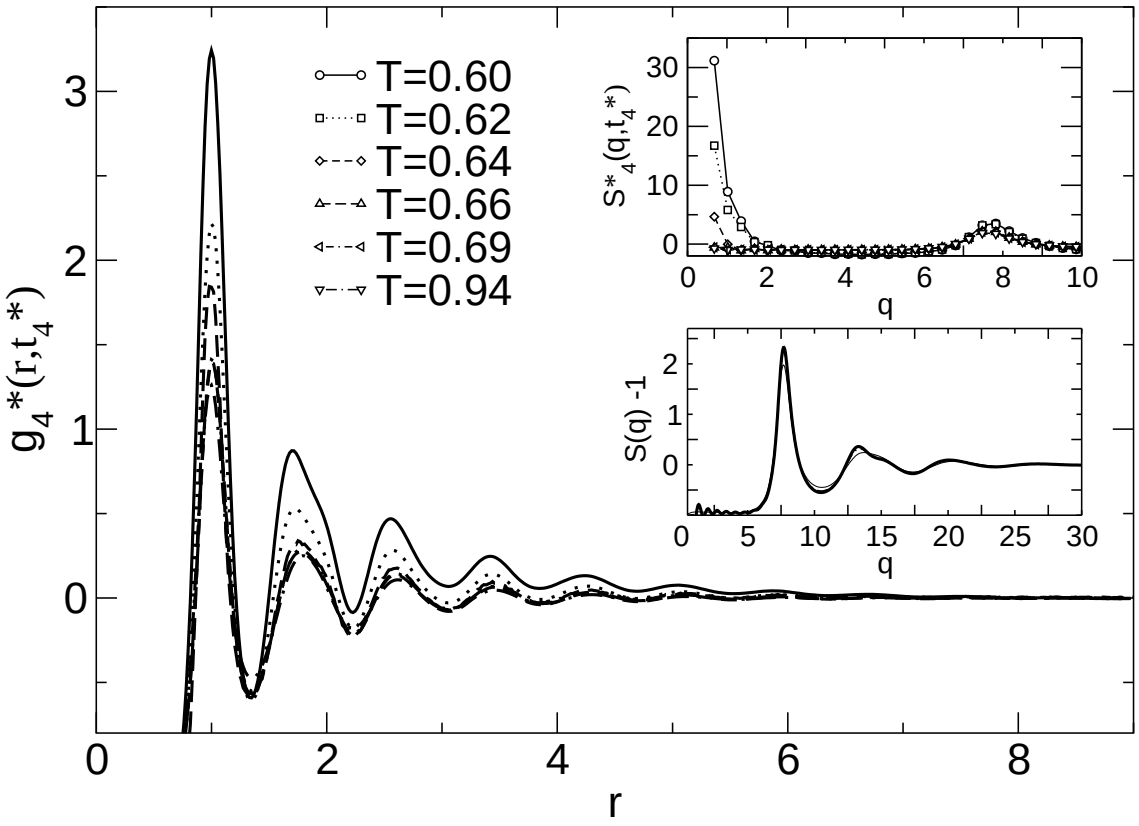

FIG. 2: Temperature dependence of $g_4^*(r,t)$ at six values of T, indicated in legend. Insets show the structure factor $S_4^*(q,t_4^*)$ and static structure factor $S(q)$ for the same values of T. We note that $g_4^*(r,t)$ is analogous to $g(r)-1$, and $S_4^*(q,t)$ is analogous to $S(q)-1$.

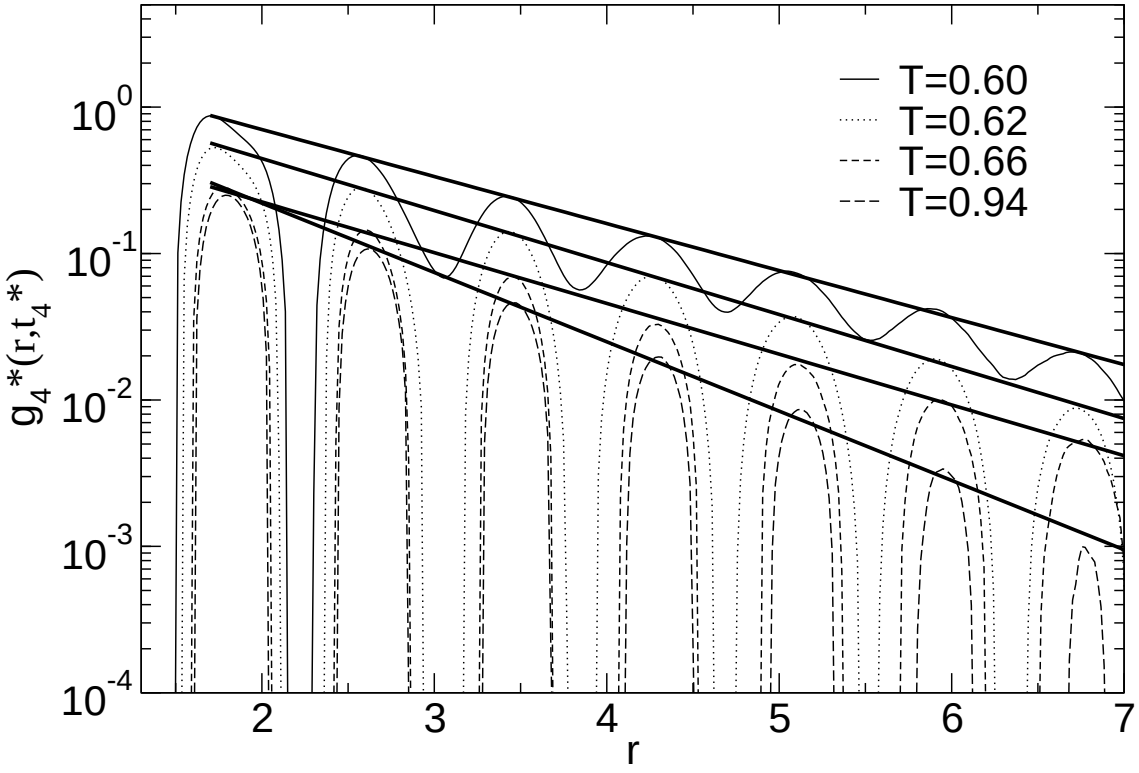

FIG. 3: Semilogarithmic plot of $g_4^*(r, t_4^*)$ in the range $1.7 < r < 7$ at four T. The solid lines are the exponential curves obtained from an "envelope fit".

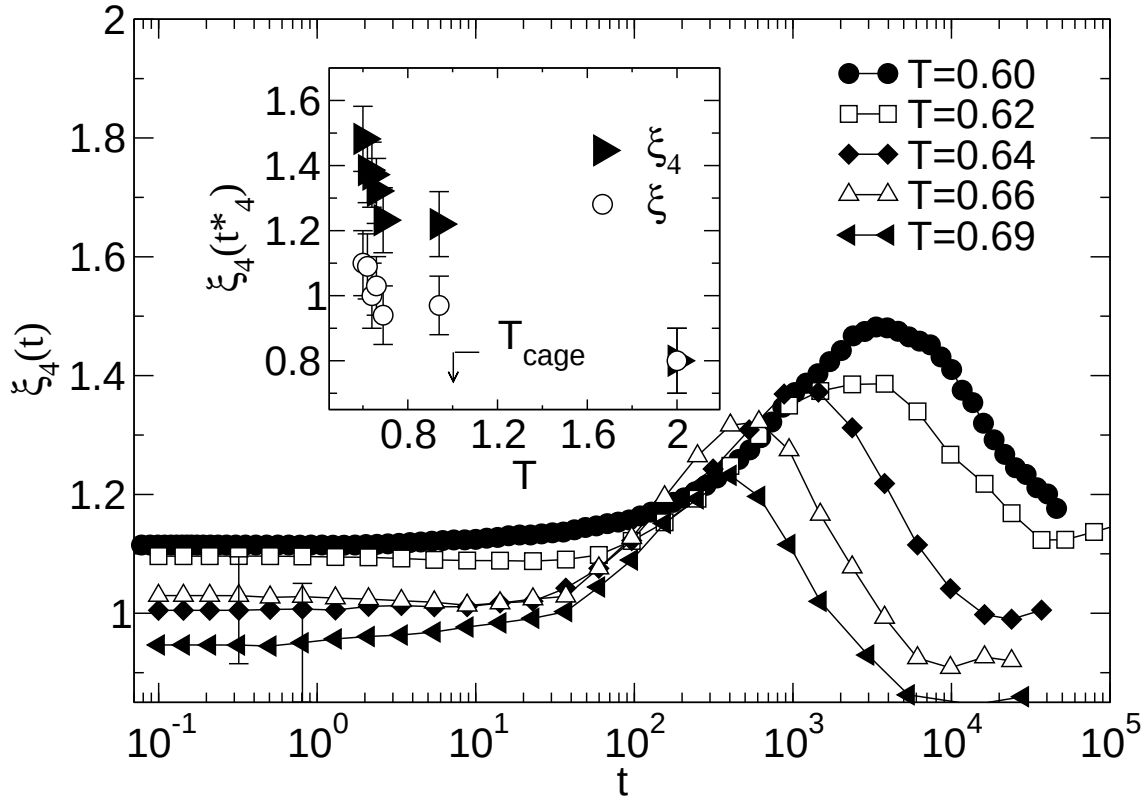

FIG. 4: Time and T dependence of $\xi_4(t)$. The inset shows $\xi_4(t_4^*)$ vs. T. The data shown is smoothed by performing running average over successive groups of five points.